Volumetric Bit-Wise Memories

T. D. Milster*, Y. Zhang*, J. Butz*, Tim Miller*, E. P. Walker**

*Optical Sciences Center
University of Arizona
Tucson, Arizona 85742
milster@arizona.edu

**Call/Recall, Inc.
6160 Lusk Blvd., Suite C-206
San Diego, CA 92121

ABSTRACT

Three-dimensional (3D) optical memory is a revolutionary technology that has the benefits of lower cost (tens of dollars/Gbit), low risk, and an order of magnitude smaller size and mass. Our research centers on a 3D optical memory device based on a new class of light-absorbing (photochromic) compounds that absorb photons two at a time when pulsed with a high-power laser, triggering chemical and physical changes with micrometer-sized resolution in three dimensions. We describe progress on media characterization at elevated temperatures and estimation of media performance based on modeling and experiment. We also describe an advanced test stand for recording and reading 2-photon media, featuring a compact design and a novel tracking servo system.

I. INTRODUCTION

This year, commercial applications will store more than two exabytes of information in digital media. Approximately 10 % of the information will be stored on magnetic disk drives, with the remainder on tapes and optical disks. This increasing capacity demand has thus far been met through steady increases in areal density of magnetic and optical recording media, where data are stored on a planar surface. While the limits of magnetic recording are still being debated – recently over 100 Gbit/in^2 has been demonstrated - the limits of conventional optical storage are well understood. New digital-video-recorder (DVR) optical storage technology is working close to the theoretical maximum areal density (15 Gbit/in^2). Future increases in density are possible by taking advantage of shorter wavelength lasers, higher lens numerical aperture, or by employing near-field techniques.[1,2] Conventional optical data storage capacities have also been increased by creating 2-layer media and bonding two such media back to back.

The three-dimensional (3D) volumetric approach to increasing effective storage capacity is quite unique for optical memory technologies. Three-dimensional storage is envisioned as a cubic storage element with bit spacing having dimensions of the writing/reading laser wavelength. Instead of recording only on a plane, bits are stored throughout the volume of the material. With a wavelength of 650 nm, storage of one terabit per cubic centimeter is possible.

We are investigating and characterizing a 3D volumetric optical memory device based on a new class of light-absorbing (photo-chromic) compounds that, when pulsed with lasers, absorb photons two at a time and can trigger chemical and physical changes (such as fluorescence) with micrometer-sized resolution in three dimensions.

Our activities aim at enabling the Earth Science Enterprise (ESE) to integrate large global data sets involving space based observation systems. With many space and ground-based sensors, ESE must acquire, process, and deliver huge volumes of data. These remote sensing and related data will help solve problems such as global change, environmental monitoring, agricultural inventory, etc.[3] The amount of data to be collected and processed per satellite runs into terabytes.

Development of adaptive, high capacity, high data rate optical storage for space vehicles can set an infusion path by establishing a realistic on-board storage platform for such data organization technologies as feature extraction and data prioritization for transmission. The impact of establishing reliable ultra high capacity storage can also significantly influence development of hierarchical data segments and reduction in data

volume for downlink. Terabyte capacity on-board optical storage is an ideal platform on which generations of data products for direct distribution to users can be made possible.

Our last report discusses details of the photochromic process, media testing and disk format.[4] The following sections provide a snapshot of our current research progress, which includes characterizing 2-photon materials for space environments and development of an engineering model. Section 2 provides background on the photochromic process. Section 3 describes our media characterization experiments and results of temperature sensitivity studies. Section 4 describes simulation of the optical readout process and results of several studies, including transfer-function characteristics, carrier-to-noise ratio versus defocus, inter-layer crosstalk, lens design issues and development of high-data-rate channels. Section 5 reports progress on the Advanced Engineering Model (AEM), which is a miniaturized test stand that includes a new servo concept. Section 6 summarizes our conclusions.

II. BACKGROUND ON THE PHOTOCHROMIC PROCESS

With a tightly focused laser beam, the photochromic process can be initiated and controlled within micrometer-size spaces. A data mark is written within the volume only at points of sufficiently high intensity.[5,6,7,8] At these points, two-photon absorption occurs, resulting in a bond dissociation. Thus, the molecular structure is changed into a new, 'written', molecule with a different absorption and emission spectrum, as shown in Fig. 1. To "read" the information written within the volume, the approach exploits the fact that the written form absorbs at longer wavelengths than the unwritten form. As shown on the right side of Fig. 1, excitation of written molecules is followed by fluorescence at ~660 nm, which returns the molecule to its ground state. The presence or absence of this fluorescence is detected and classified as a physical '1' or '0' for the stored data mark. Since the decay lifetime is ~5 nanoseconds and the concentration of molecules is high, it is possible to excite the written molecules many times in a single read cycle and increase the total light collected at the detector.

The advantage of a 2-photon absorption process is based upon its ability to selectively excite molecules inside a volume without populating molecules on the surface of the device. This may be achieved because the laser photons have less energy than the energy gap between the ground state and first allowed electronic level. Therefore, photons propagate through the medium without being absorbed by a one-photon process. However, in the vicinity of the laser beam focus, the intensity is high enough so that two photons can combine to excite carriers across the energy gap. The transition probability of a 2-photon absorption process partly depends upon the writing beam intensity, so lasers emitting high intensity light in short pulses, i.e. picosecond and sub-picosecond pulses, must be used.

The recording material is dispersed in a polymer host, which can then be shaped to produce disks with integrated structures for alignment and mounting. This project uses 25mm x 3mm PMMA disks with homogeneously dispersed storage materials. Polymerization molding, compression molding and polishing have been utilized to produce the desirable optical quality polymer for 3D optical memory disks.

A representation of the disks we use is shown in Fig. 2, where other technologies are also shown for comparison. Our 25 mm diameter test samples, if used with 500 layers and 1 Gbyte per layer, can produce a disk containing 500 Gbytes. With parallel readout beams, high data rate retrieval can also be achieved.[9]

III. MEDIA CHARACTERIZATION EXPERIMENTS

The recording material is an essential element in an optical data storage system. Both behavior of materials currently being used and characterization of promising new materials are measured in this study. To date, temperature study results indicate various characteristics about the particular 2-photon material and substrate used in our experiments. Also, no new materials with strong nonlinear absorption are identified.

In order to study the temperature dependence of 2-photon disks in a space environment, a vacuum oven is used to heat pre-written disk substrates at temperatures from 50C to 90C in a 10^{-3} torr atmosphere. After being removed from the oven and allowed to cool, readout signals are evaluated on the Arizona Readout Test Stand (ARTS), which is shown in Fig. 3. ARTS is a dedicated test stand that measures readout signal quality from 2-photon fluorescent media. ARTS is described in our previous paper in some detail.[4,10]

A critical temperature envelope of 1.5 hours at 70C or 1.0 hour at 80C exhibited approximately a 50%

failure rate in the disks. Interestingly, disk failure is not due to intrinsic photochromic damage. For example, Fig. 4(a) shows a CCD image of bits inside the disk before heating. Fig. 4(b) shows a typical image of bits inside the disk after heating. There is no visible degradation of fluorescence between Figs. 4(a) and 4(b). Figure 5(a) shows the time-domain readout signal before heating, which exhibits a straight baseline and large signal amplitude. Figure 5(b) shows the time-domain readout signal after heating, which exhibits a strongly curved baseline without a significant reduction in signal amplitude. A curved baseline is indicative of a servo error, where ARTS is not able to follow the data track sufficiently well as the disk spins during readout. CCD images in Fig. 4 and signal amplitudes in Fig. 5 indicate that the intrinsic photochromic properties of the medium are not significantly affected in this temperature range.

In order to identify cause of the servo error, the front surface of the disk is examined with a Ronchi test.[11] Figure 6(a) shows the front surface of the disk before heating. Ronchi lines are patterns of dark fringes covering the surface. If the surface is perfectly flat, Ronchi lines are straight and equally spaced. Magnitude of surface departure is proportional to displacement of fringes from the straight pattern. In Fig. 6(a), fringes are mostly straight, except near edges and near the center mounting hole. In Fig 6(b), which shows the disk surface after heating, a significant distortion of the surface is apparent.

We conclude that disk failure is due to a servo error caused by deformation of the molded PMMA disk substrate. Operation of disks at or above the critical temperature envelope requires development of a more robust substrate material that can withstand higher temperature ranges.

IV. DATA CHANNEL DEVELOPMENT

Several important characteristics of volumetric recording systems are investigated with simulation tools. Data from these calculations are used to compare different readout systems and to characterize performance parameters, like carrier-to-noise ratio versus defocus and inter-layer crosstalk.[12] In addition, information about optical system design helps us to understand realistic limits of volumetric recording. The following sections describe transfer-function characteristics of confocal and nonconfocal readout, focus sensitivity based on carrier-to-noise ratio (CNR), acceptable operating regions based on interlayer crosstalk, and maximum volumetric density and effective surface density for two types of readout optical systems. High data-rate channels are also introduced.

Transfer function characteristics of confocal and nonconfocal readout systems

Figure 7 shows a volumetric read out system. The incident laser beam is focused onto a bit plane of interest. The distance between marks in the same bit plane is T_x, while the distance between two bit planes is T_z. Spatial frequency is defined as $f_x=1/T_x$, $f_y=1/T_y$ and $f_z=1/T_z$. The 3-D OTF for a fluorescent system is defined as:

$$I(x',y',x_s,y_s,z_s)= O(f_x,f_y,f_z)*OTF(f_x,f_y,f_z,x',y') *\exp(-i*2*\delta*(f_x*x_s+f_y*y_s+f_z*z_s))df_x\,df_y\,df_z, \quad (1)$$

where I is the irradiance distribution on the imaging plane.[13,14,15,16,17]

Both confocal type and non-confocal type read out systems are simulated. The confocal read out system uses a pinhole with a radius of one micron, while the non-confocal read out system uses a pinhole with radius of one hundred microns. In both simulations, we assume that the numerical aperture (NA) of the objective lens is 0.6, the incident laser wavelength is 635nm, and the fluorescent wavelength is 675 nm. The NA (numerical aperture) of an objective lens is defined as the sine of the angular semi-aperture in image space times the refractive index of image space. Larger NA leads to smaller spots and shorter depth of focus. The fluorescent light is focused onto a detector on which a pinhole is mounted.

The simulation shows that in both cases the 3-D OTF has the same cut-off frequency in the (fx, fy, fz) domain. Simulation results are shown in Fig 8(a),(b),(c). In Fig 8(a), the dashed curve represents the relative power spectrum profile of a confocal system along the fz axis, while the solid curve represents the relative power spectrum profile of a non-cofocal system along the fz axis. This curve demonstrates that the non-confocal case has a higher power spectrum.

Figure 8(b) shows the OTF profile of a confocal system along the fx axis. The solid curve is the OTF distribution on the plane where fz = 0, and the dashed curve is the OTF distribution on the plane where $fz = 0.4 \times NA^2/\lambda$. Notice that the OTF profile along the fx axis depends dramatically on fz.

Figure 8(c) shows the OTF profile of a non-confocal system along the fx axis. The solid curve is

the OTF distribution on the plane where fz = 0, the dashed curve is the OTF distribution on the plane where fz = 0.4 x NA^2/λ. Again, the OTF profile along the fx axis depends dramatically on fz. This curve also shows that the confocal system can pass all the low frequency information in a specific fz plane, while the non-confocal system will block some low frequency information in a specific fz plane.

.

Focus sensitivity of one layer

The focus sensitivity of one layer for both confocal and non-confocal read out systems is simulated by applying the 3-D OTF. The same specifications of a confocal and non-confocal read out system are adopted in this simulation. Nine different sizes of marks are used, and the 3 dB focus range is calculated for each size. Simulation results are presented in Table I. Results demonstrate that CNR of a confocal system is at most 3 dB lower than CNR from a non-confocal system. The 3 dB focus range is almost the same as the mark depth in a non-confocal system, while it is slightly smaller in a confocal system. Results also show that longer marks result in higher CNR.

Acceptable region of operation based on inter-layer crosstalk

Figure 9 is the general diagram of mark patterns used to simulate inter-layer crosstalk. Marks in the upper and lower layers are 3x3x15 microns with 50% duty cycle. Marks in the middle layer are 1.5x1.5x15 microns with 50% duty cycle. This simulation studies the crosstalk level of the upper and lower layer signals present while reading the central layer. Parameters include Δz and Δb. An acceptable region of operation is based on inter-layer crosstalk for both confocal and non-confocal readout systems. Δz is the distance between the center of the layer and the focal plane of the incident laser beam. Δb is the layer-to-layer distance. Figure 10 (a) and (b) show contours of inter-layer crosstalk level versus Δz and Δb for non-confocal systems and confocal systems, respectively. The shaded area is the acceptable region of operation based on a –30 dB crosstalk criterion. Our simulations show that the confocal system significantly reduces the inter-layer crosstalk level. Hence, the non-confocal system needs tighter focus control for smaller crosstalk and maximum volumetric density. The significantly reduced inter-layer crosstalk level and minimal 3 dB CNR penalty suggest that the confocal system should be used for this two–photon read out system.

Lens design study to determine realistic volumetric and effective surface density

The are two kinds of objective lenses used for single-layer data storage systems. One is a low NA lens, which is similar to a Geletch lens with 0.55 NA.[18] The other one is a solid immersion lens (SIL), which uses a hemispherical lens in close proximity to the medium, which increases the system's numerical aperture (NA) to a typical value of 1.2.[1] In order to apply these lenses into a multiple-layer data storage system, proper compensators are needed because of spherical abberation (SA) generated by the focus moving through different layers,[19,20] as shown in Fig 7. In this study, a Galilean telescope compensator with magnification of 2.0x is optimized for multiple layer read out. Figure 11 shows layout of a multiple layer low NA read out system using the Galilean telescope compensator combined with a Geltech objective lens. Focus performance is checked at specific focus depth positions and presented in Table 2. The study shows that there is 2 mm allowable focus depth range within 90% Strehl ratio and less than 0.05 wave RMS wave-front aberration error. If the bit cell is 1 x 1 x 10 micron, the maximum number layers of data inside a disk is 200, and the volumetric storage density will reach 10^{11} bits/cm^3. The surface storage density using this low NA system will reach 2 x 10^{10} bits/cm^2.

To achieve ultra high density optical data storage, a diffraction limited high NA optical system using a SIL lens is needed. Layout diagram of an optimumized SIL system is shown in Fig 12. The effective focal length of this system is 1.15 mm with 1.2 NA. The off-axis field angle is optimized at 0.5 degree. Table 3 shows the focal performance data as a function of media thickness. This simulation suggests that there is 200 micron allowable focus depth range within 80% Strehl ratio and less than 0.07 wave RMS wave-front aberration error. If the bit cell is 0.5x0.5x2 micron, the maximum number of layers is 100, and the volumetric storage density will reach $2x10^{12}$ bits/cm^3. The surface storage density using this kind of low NA system will reach $4x10^{10}$ bits/cm^2. Overall, the high NA system provides a compact and high storage density solution.

High data-rate channel

To achieve a high speed data channel, Call/Recall has developed and demonstrated a parallel readout architecture where data tracks are read in parallel across multiple layers in depth, as well as across a number of radial tracks.[9] Multiple layers of 0.7×0.7×10 micron bits are written into the volumetric media. A cross section of data observed with a profiling microscope shown in Fig 13. For high data-rate readout, a grating is used to generate a two dimensional focused spot array that illuminates the bits inside a disk so that multiple tracks within multiple layers are read simultaneously. A doubly telecentric afocal system is designed to image the data bits to a detector array. Fig 14 shows the experimental setup of a 4(layer) x 16(track) multi-channel read system. The inter-track and inter-layer crosstalk measured on this test stand is 25-30 dB lower than CNR of the fundamental frequency, indicating good performance of this 64 channel read out system.

V. ADVANCED ENGINEERING MODEL (AEM)

Although ARTS and similar test stands are very useful for characterizing media and basic concepts of three-dimensional storage, size and complexity of these test stands are impractical to fly in spacecraft. The Advanced Engineering Model (AEM) is a miniaturized test stand that is a first step toward a flyable two-photon optical device. AEM incorporates readout features of ARTS with the addition of dynamic writing capability. AEM uses an advanced servo scheme for control of data mark position inside the three-dimensional volume.

Basic optical paths of the AEM are shown in Figs 15(a) and (b). In the write path, a high-power 532 nm laser is directed off a dichroic beam splitter and through the objective lens into the medium. In the read path, a low-power 638 nm laser diode illuminates the data mark pattern through the beam splitters and objective lens. Fluorescent light with a center wavelength of 650 nm is directed through the first beam splitter and off the second beam splitter to the detector. In this AEM, we implement only a single-beam optical system. However, our plans include a multiple-beam version in the near future.

A distinct advantage of the three-dimensional media concept presented here is that the media are simple homogeneous molded disks. That is, there is no complicated multilayered structure required in the disk during fabrication. Therefore, media are very economical. However, since disks are homogeneous, there are no reference features to guide the laser beam during recording or readout. Some type of reference signal is necessary, because variations in spindle rotation and disk thickness cause position errors many times the size of the focal region as the disk rotates. In conventional CD or DVD disks, a reference signal is provided by grooves aligned with data tracks. To date, the only method for keeping the beam aligned in three-dimensional media is to servo from a signal generated from the data itself.[21]. Although this method produces good results, writing data is performed open loop. Therefore, interchangeability between players may be problematic.

An interesting servo concept called "slave servo" is applied to the AEM in order to control focus position within the three-dimensional volume. As shown in Fig. 16, a master disk is rigidly attached to a disk containing three-dimensional data. In our first prototype, the master disk is a simple unwritten CD-R disk. The three-dimensional data disk is a 25 mm diameter photochromic media sample from Call/Recall, Inc. The master disk is used to provide a reference signal for the slave actuator in the optical head that focuses laser light into the three-dimensional medium.

A reference signal is generated from an off-the-shelf CD optical head. As the master disk spins, error signals are generated from the detectors inside the head that are used in a servo loop to control tracking and focus position of the CD objective lens. As the objective lens moves, the laser spot from the CD head is repositioned correctly to follow tracks on the master disk. This same error signal is processed by the electronics and is used to position the objective lens that focuses light into the three-dimensional medium. The processed error signal is called the "slave servo signal". As the disk spins, the slaved objective lens repositions itself according to same correction required in the master disk. Therefore, position errors due to motor or disk dynamics are minimized. Repeatable and accurate positioning of the slaved lens and laser beam should result. An electrical offset is provided to the slave servo, so that multiple focal planes can be accessed in the three-dimensional medium.

The AEM prototype is shown in Fig. 17. The read-laser head is a modified commercial head that was originally used in an optical library product. Beamsplitters are housed in rectangular mounts

between the read-laser heads and the slave objective lens. The two-photon d
isk is bonded to the master disk, which is a commercial CD-R. The spindle motor and off-the shelf CD head are mounted behind the master disk. Servo electronics are mounted separately. Physical size of the first AEM is only 17.5 cm by 10 cm by 10 cm. Future versions of the AEM could be packaged into volumes as small as 5 cm by 10 cm by 5 cm.

VI. SUMMARY AND CONCLUSIONS

We investigate and characterize the properties of 2-photon volumetric media, through experiments and modeling. Experiments show that current recording materials operate well up to 70°C. Above this temperature, substrate deformation causes a failure in the servo's ability to focus, although evidence of normal fluorescence suggests that the photochromic process is unaffected. We model the volumetric recording process to estimate various performance parameters. We find that a layer thickness of 10 microns has an acceptable CNR, and leads to a volumetric density of 10^{11} bits/cm^3. This layer thickness is demonstrated experimentally. A maximum volumetric density of 2×10^{12} bits/cm^3 can be accomplished using a near-field optical system. A 64-channel readout system has successfully demonstrated the potential for high-speed data retrieval with the photochromic process. We describe the design of a recordable/readable prototype unit, with construction in progress. The unit features off-the-shelf parts, a novel servo system that allows reliable tracking and interchangeability, and a compact design suitable for space flight application In summary, 2-photon data storage offers a tremendous improvement in capacity and other factors important for space applications. Our research is highly leveraged from other efforts in this area, and we are developing the technology through our understanding of media characteristics, simulations, and experiments.

ACKNOWLEDGEMENT

This work is supported through a contract from the National Aeronautics and Space Administration, contract # NAS2-00117.

REFERENCES

[1] B.D.Terris *et al*., "Near-field data storage using a solid immersion lens", *Appl. Phys. Lett*. Vol 65 (1994) No 4, pp388-390

[2] T.D.Milster, "Near-field optics: A new tool for data storage," *Proc. IEEE*, 88(9), pp 1480-1490 (2000)

[3] "Earth Science Enterprise: Strategic Plan," November, 2002, NASA Headquarters Washington, DC 20546, http:// www.earth.nasa.gov

[4] Tom D.Milster *et al*., "A Volumetric Memory Device based on Photo-Chromatic Compounds*" NASA earth science technology conference* 2001

[5] S. Hunter *et al.*, "Potentials of two-photon 3-D optical memories for high performance computing," *Appl. Opt.* **29**, pp. 2058-2066 (1990).

[6] D.C. Hutchings *et al.*, "Kramers-Kronig relations in nonlinear optics," *Optical and Quantum Electronics* **24** pp. 1-30 (1992).

[7] E. W. Van Stryland *et al.,* "Characterization of nonlinear optical absorption and refraction," *Prog. Crystal Growth and Charact.* **27**, pp. 279-311 (1993).

[8] H. Zhang *et al.,* "Single-beam two-photon-recorded monolithic multi-layer optical disks," *ODS 2000* Proc. SPIE 4090 pp. 174-178 (2000).

[9] Ed Walker *et al.,* "3-D parallel readout in a 3-D multilayer optical data storage system" *ISOM/ODS/2002*, details will be presented to ISOM/ODS 2002 conference

[10] D. Felix, T. D. Milster, C. J. Burkhart, J. Curtis, "Semi-kinematic rails for construction of optical testbeds," *SPIE -The International Society of Optical Engineering - Annual Meeting,* San Diego, California, 29 July to 3 August, 2001, paper 4444-41.

[11] Daniel Malacara, "Optical Shop Testing" Wiley series in pure and applied optics, 2nd edition

[12] T. D. Milster, "A user-friendly diffraction modeling program," Optical Data Storage Topical Meeting ODS, Conference Digest, IEEE. 109, pp. 60-71 (1997).

[13] C.J.R.Sheppard *et al.,* "Three-dimensional imaging in a microscope*" J.Opt.Soc.Am.A* Vol.6, No.9 Sep. 1989 pp1260-1269

[14] C.W.McCutchen, "Generalized aperture and the three-dimensional diffraction image," *J.Opt.Soc.Am*. 54, 240-244(1964)

[15] E.Wolf, "Three-dimensional structure determination of semi-transparent objects from holographic data," *Opt.Commun*. 1, 153-156 (1969)

[16] B.R.Frieden, "Optical transfer of a three-dimensional object," *J.Opt.Soc.Am*.57,56-66 (1967)

[17] N.Streibl, "Three-dimensional imaging in a microscope," *J.Opt.Soc.Am*.A2,121-127(1985)
[18] http://www.geltech.com; product number Geltech 350340
[19] Tom D. Milster *et al.,* "Objective lens design for multiple-layer optical data storage," *Opt.Eng*.38(2) 295-300
[20] Ed Walker *et al.,* "Spherical aberration correction for two-photon recorded monolithic multiplayer optical data storage" *Optical data storage topical meeting* 2001 154-156
[21] Ed Walker *et al.,* "Servo Error Signal Generation for 2-Photon Recorded Monolithic Multilayer Optical Data Storage," *ODS 2000* Proc. SPIE 4090 pp. 179-183 (2000).

Table I Simulation results of focus sensitivity for both confocal and non-confocal system 3dB focus range is the same as mark depth (confocal slightly lower) Results are not a strong function of mark size Largest CNR is with the deepest marks

Confocal (detector = 1μm)

Mark size (μm)	Mark depth (μm)	CNR at Δz=0	3dB range (μm)
1	1	23.0	2.15
	5	26.7	4.99
	15	26.7	14.8
2	1	23.4	2.11
	5	27.0	5.0
	15	27.1	14.9
3	1	23.4	2.14
	5	27.1	5.0
	15	27.2	14.9

NonConfocal (detector = 100μm)

Mark size (μm)	Mark depth (μm)	CNR at Δz=0	3dB range (μm)
1	1	24.1	3.68
	5	29.7	5.43
	15	30.7	14.88
2	1	24.6	3.24
	5	29.3	6.71
	15	30.5	15.03
3	1	24.6	3.27
	5	29.3	6.84
	15	30.6	16.22

Table 2 Focus performance data for Galilean telescope SA compensation system / NA=0.6.Allowable focus range is 2mm. T_{media} is the distance between the front surface of the disk and the focal plane of incident laser beam. T_{zoom} is the distance between two lenses of the Galilean telescope compensator. T_{focus} is the working distance of the objective lens.

T_{media}	T_{zoom}	T_{focus}	$Wave_{error}$	Strehl(%)
0.1mm	1.145	2.394	0.048	91
0.4	1.075	2.232	0.025	98
0.8	1.012	2.070	0.007	100
$1.2_{nominal}$	1.533	1.668	0.002	100
1.6	2.435	1.224	0.014	99
2.0	3.735	0.771	0.035	96
2.4	4.536	0.458	0.128	52

Table.3 Focus performance data for optimum-SIL system / NA=1.2 Allowable focus range is 200μ. ΔTz is the distance between two lenses of the compensator ΔSIL+d is the distance between the front surface of the SIL and the focal plane of the incident laser beam

ΔTz(mm)	ΔSIL+d (micron)	ΔWave front	Strehl(%)
0.31	-70	0.08	79/76
0.22	-50	0.07	82/81
0.00	0	0.07	85/83
-0.20	45	0.07	82/81
-0.44	100	0.06	88/86
-0.56	130	0.06	91/82

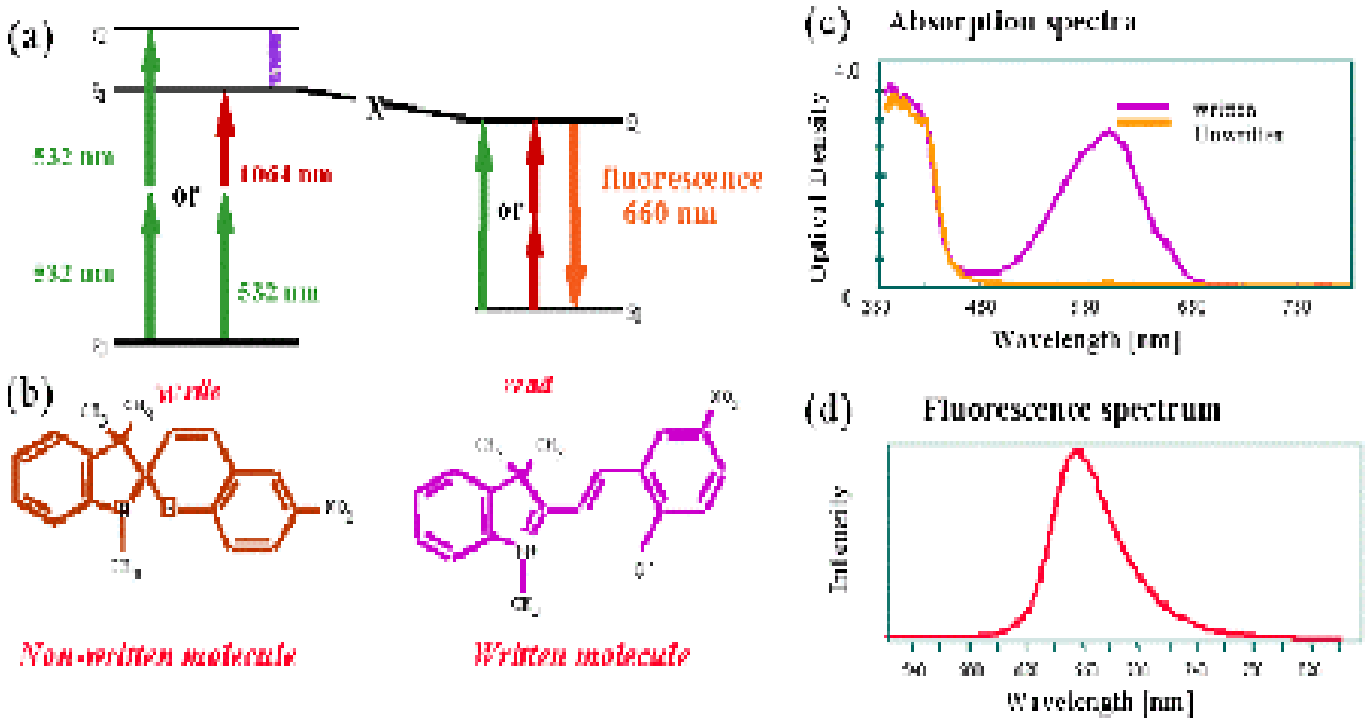

Fig. 1represents a physical description of what happens when two-photon absorption occurs. (a) Energy-level diagram of unwritten and written forms, showing fluorescence; (b) structure of an unwritten molecule and a written molecule (c) absorption spectra of the unwritten and written forms of the material (d) fluorescence spectrum of the excited written form

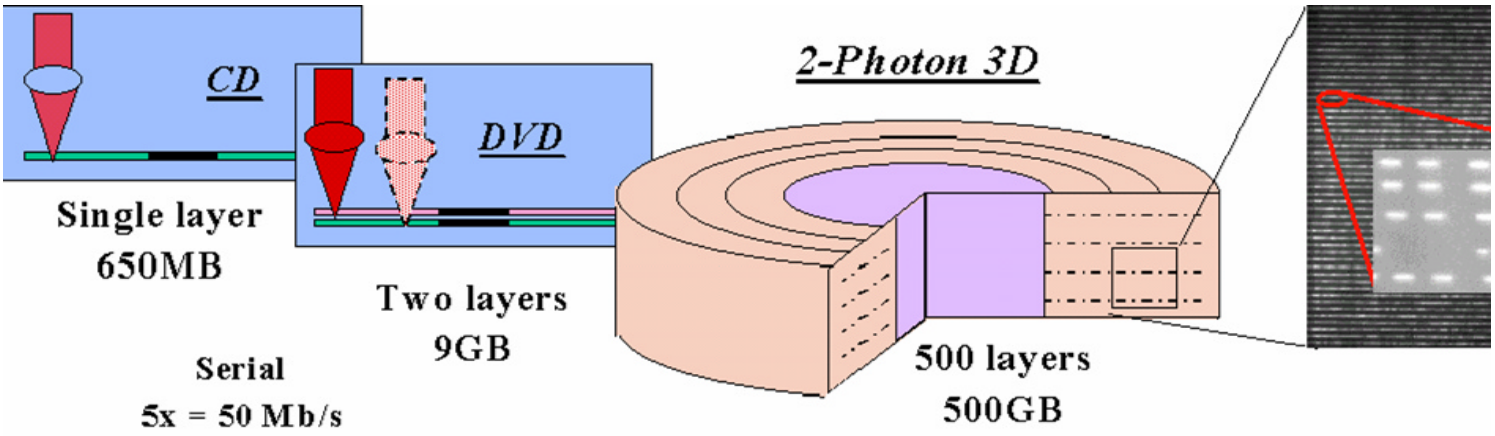

Fig 2 Two-photon #D disk media samples used in this study are 25 mm in diameter and 3 mm thick. If 500 layers are used, the storage capacity could be 500 Gbytes. High data-rate channels could provide up to 500 Mbits/sec data rate. CD and DVD are shown for comparison.

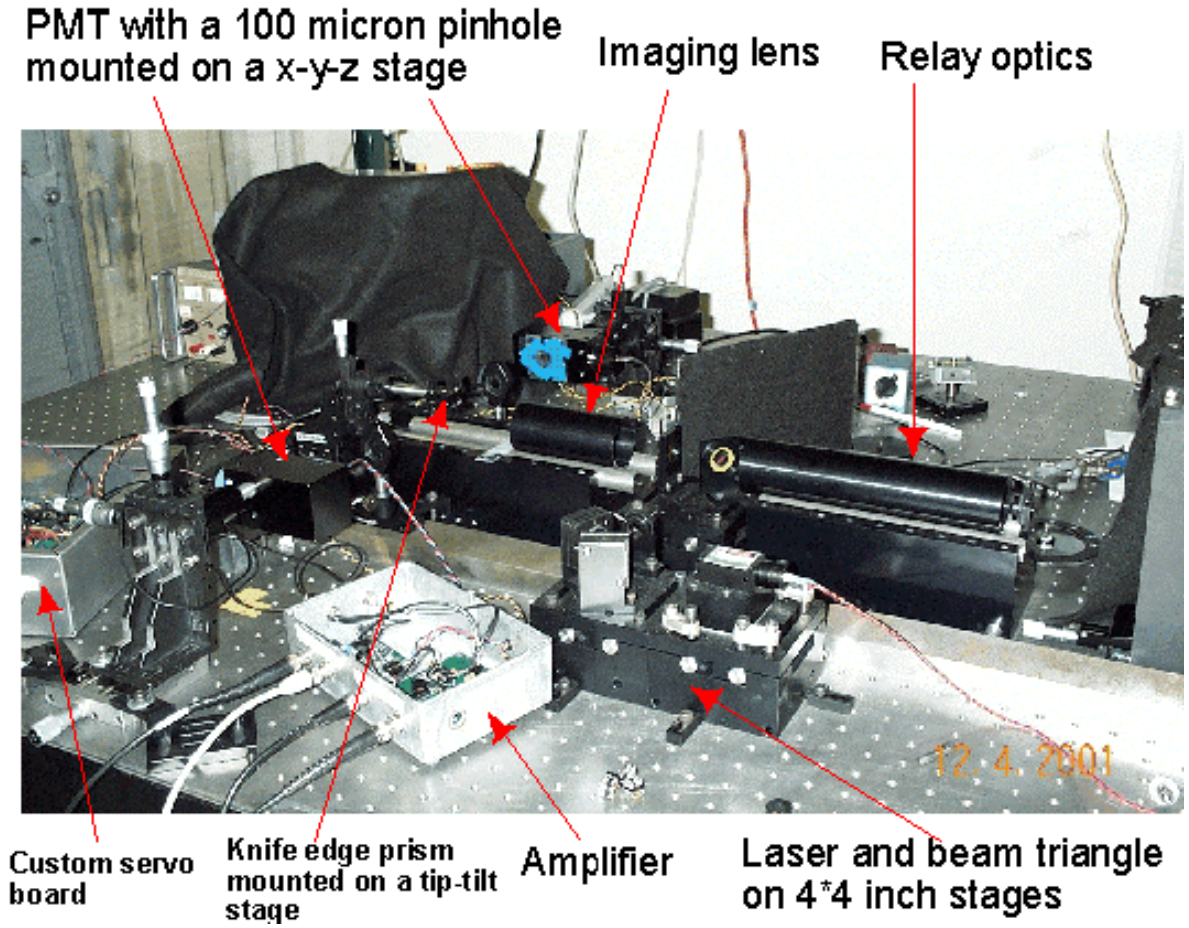

Fig 3 Arizona Readout Test Stand (ARTS). ARTS is a dedicated test stand that measures readout signal quality from 2-photon fluorescent media. A laser diode is imaged into the spinning volumetric medium after being relayed through custom optics. Dichroic beamsplitters and the imaging lens direct light from fluorescent bits onto a knife-edge prism that splits the beam onto two PMT detectors with pinholes. Custom electronics, including amplifiers and servo loops, enable the system to lock the focus beam onto a data track and produce a high-quality readout signal as the disk spins.

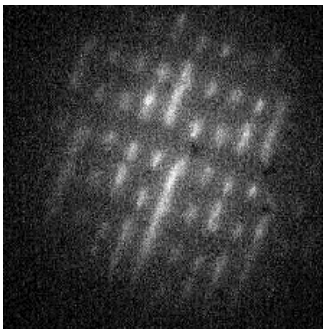

Fig 4(a) CCD image of fluorescent bits before heating.

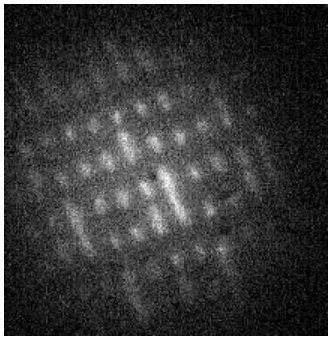

Fig. 4(b) CCD image of fluorescent bits after heating. No apparent change is observed compared to Fig. 4(a).

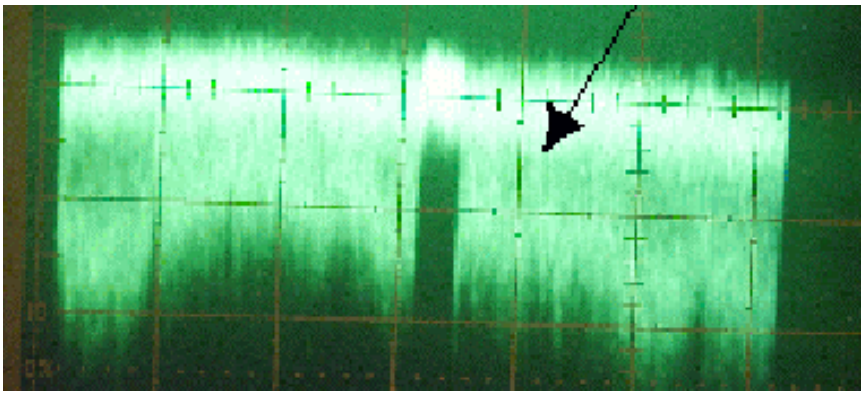

Fig 5(a) Time domain readout signal before heating exhibits a straight baseline and large signal amplitude.

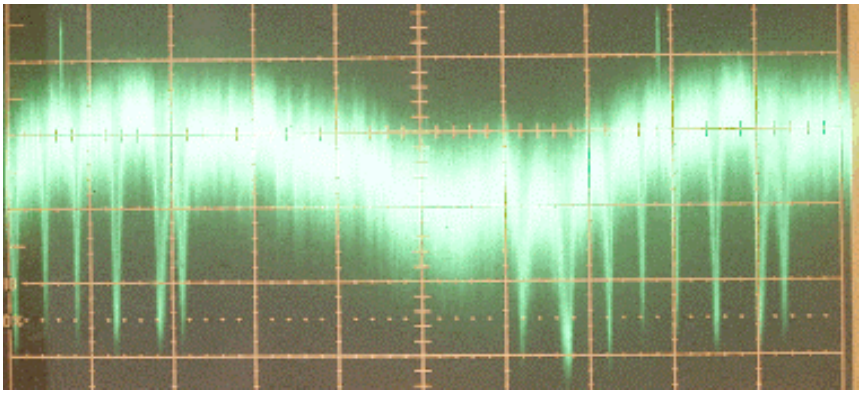

Fig 5(b) Time domain readout signal after heating exhibits a strongly curved baseline, without a significant reduction in signal amplitude.

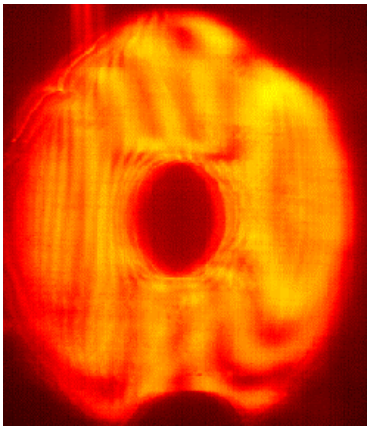

Fig. 6(a) Ronchi test interferogram of the disk front surface before heating. Straight lines indicate a relatively flat surface

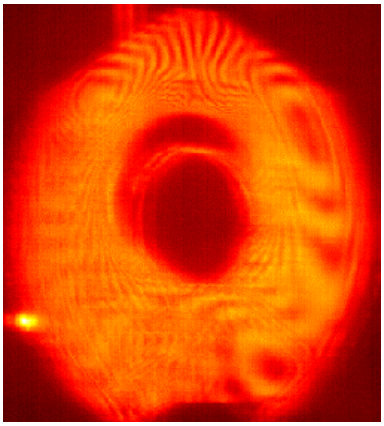

Fig. 6(b) Ronchi test interferogram of the disk surface after heating. Complex line patterns indicate a deformed surface.

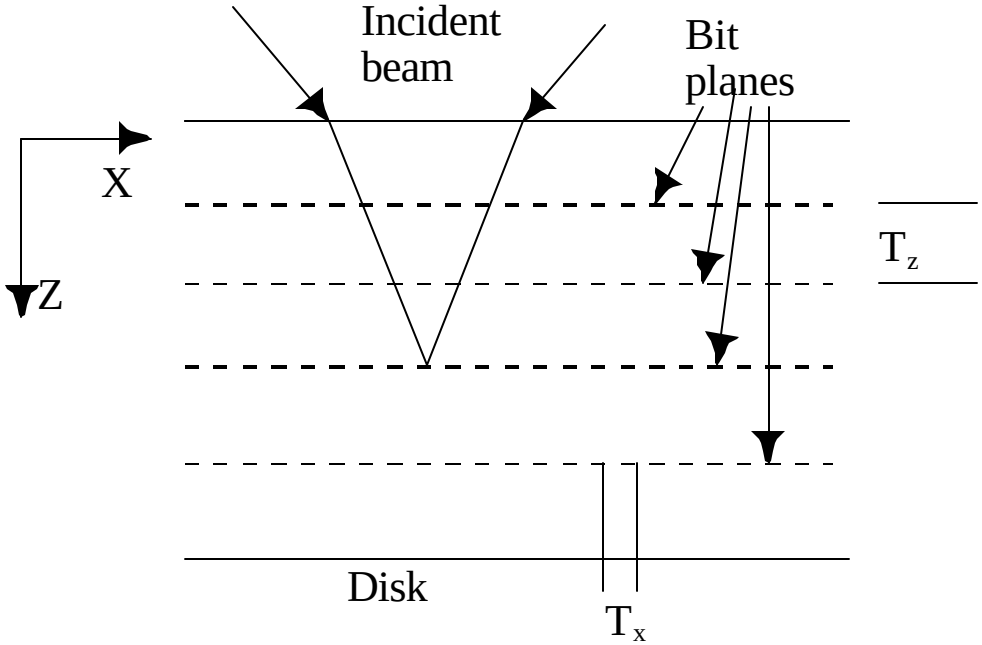

Figure 7 A typical volumetric read out system. The incident laser beam is focused onto a bit plane of interest. The distance between marks in the same bit plane is T_x, while the distance between two bit planes is T_z.

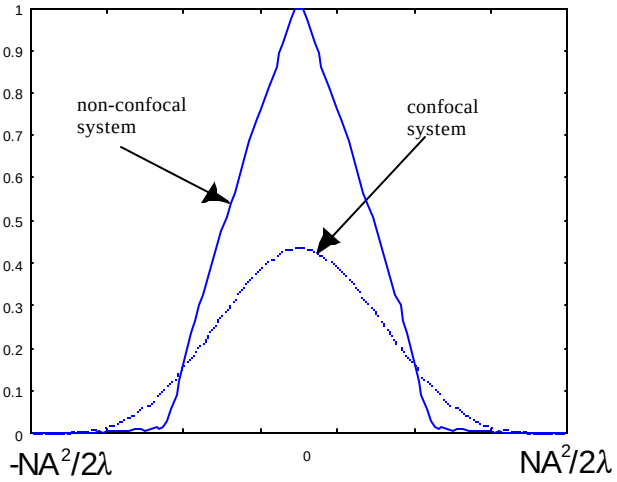

Fig 8a Relative spectral power profile of two optical transfer functions (OTFs)along the fz axis

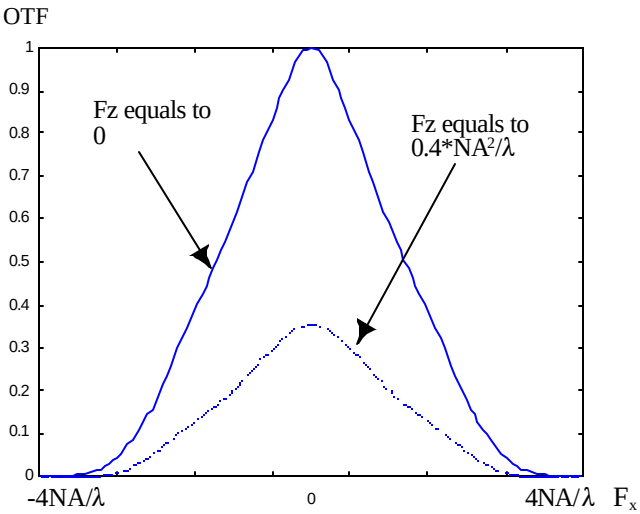

Fig 8b OTF profile of an incoherent confocal system on two fz planes

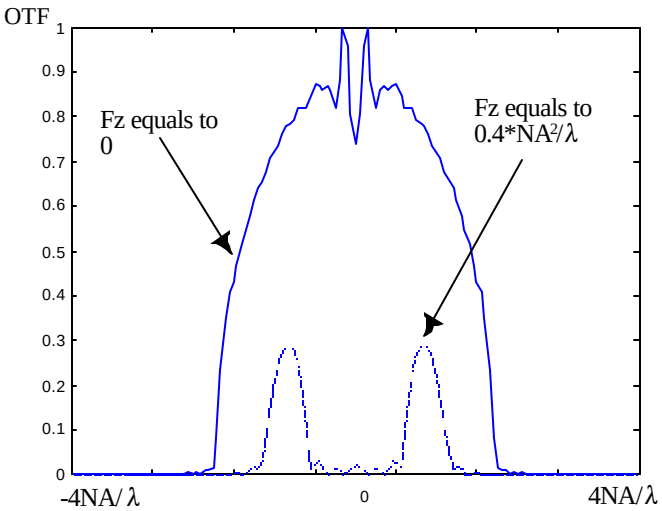

Fig 8c OTF profile of an incoherent non-confocal system on two fz planes

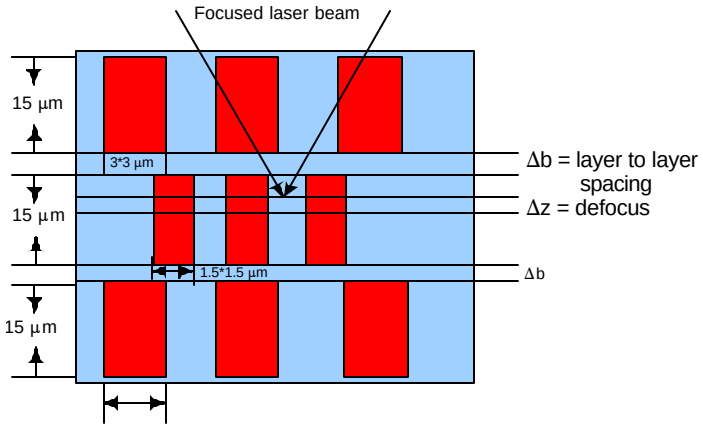

Fig 9 Mark patterns used to simulate inter-layer crosstalk.

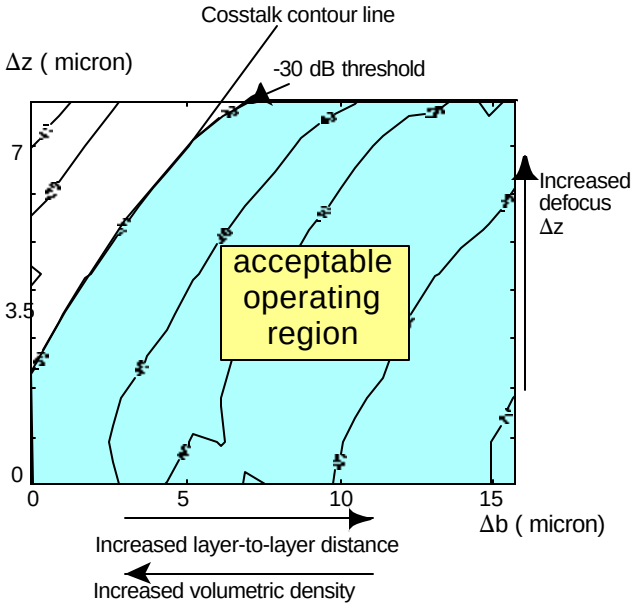

(a)

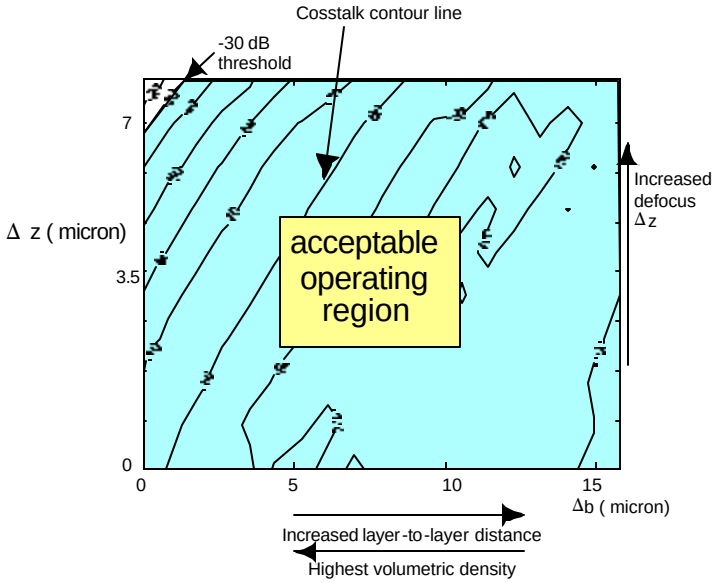

(b)

Fig 10 Contours of inter-layer crosstalk level versus Δz and Δb for (a) non-confocal systems and (b) confocal systems. The shaded area is the acceptable region of operation based on a –30 dB crosstalk criterion. The confocal system has the largest acceptable operating region.

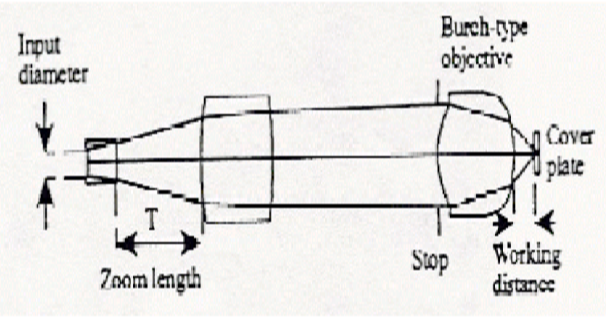

Fig 11 Layout of a multiple layer low NA read out system using the Galilean telescope compensator combined with a Geltech objective lens.

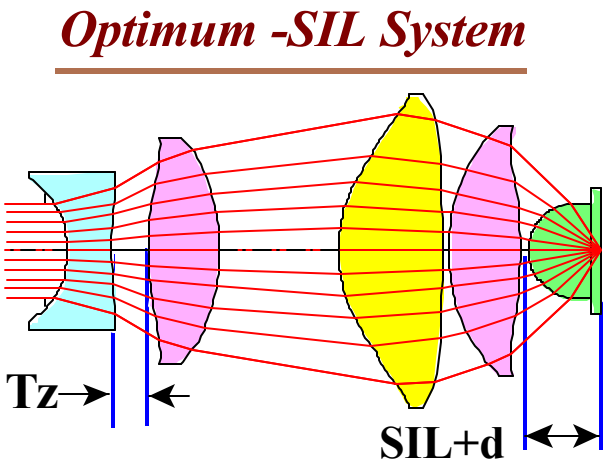

Fig 12 Layout of a diffraction-limited high NA optical

system using a SIL lens.

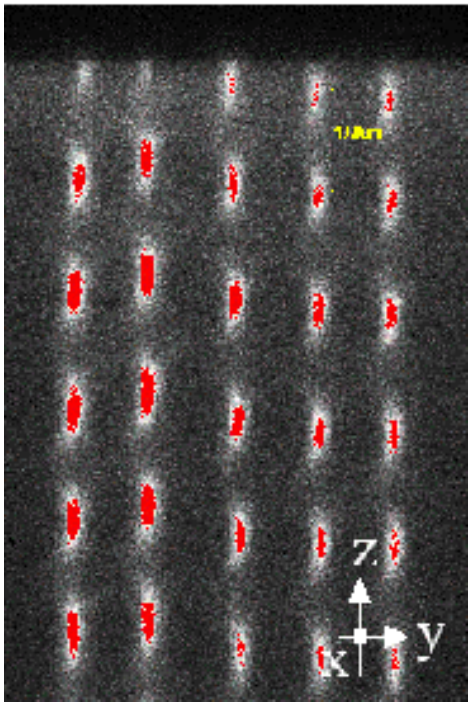

Fig 13 .A cross section of multiple layers of fluorescent bits (0.7×0.7×10 micron bits) written into volumetric media, observed with a profiling microscope CCD.

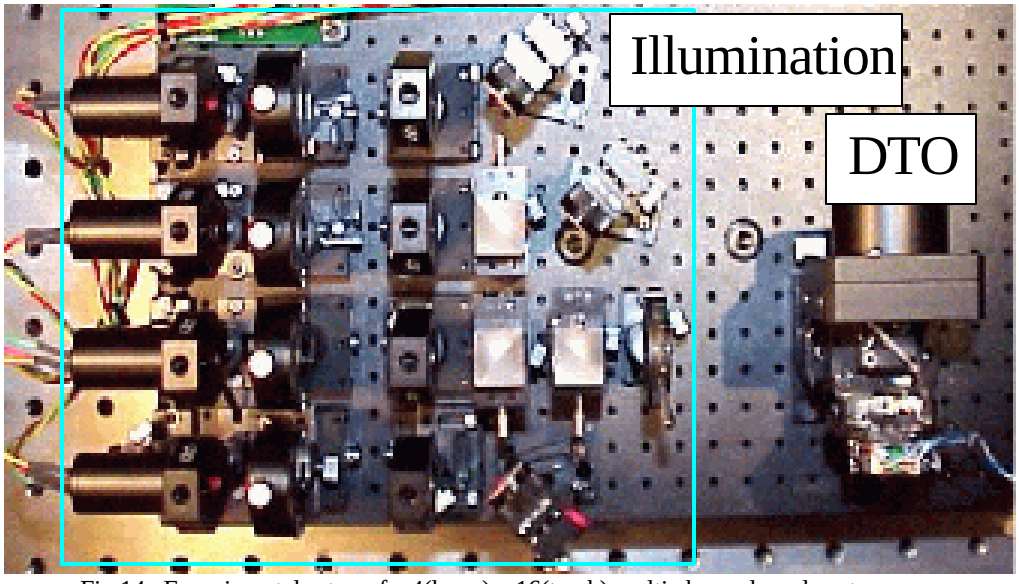

Fig 14 Experimental setup of a 4(layer) x 16(track) multi-channel read system.

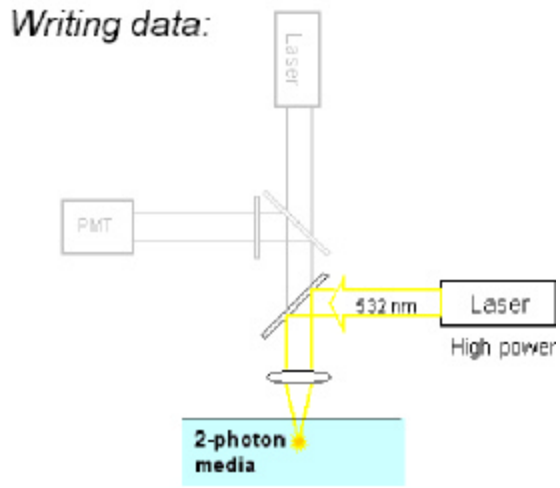

Fig 15(a) Write path of Advanced Engineering Model (AEM). A high-power 532 nm laser is directed off a dichroic beam splitter and through the objective lens into the medium.

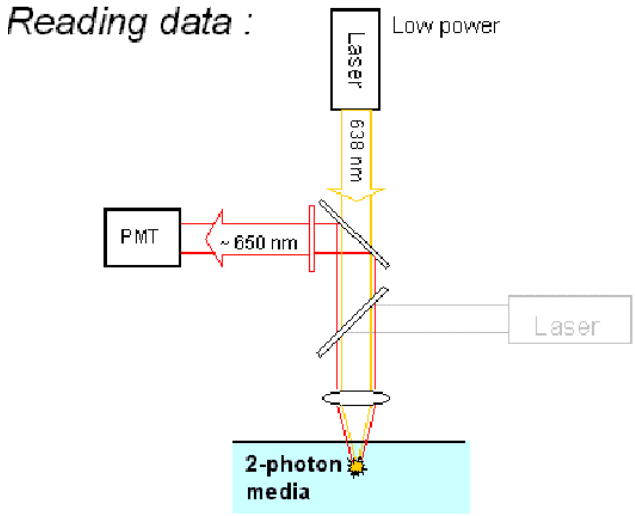

Fig 15(b) Read path of Advanced Engineering Model (AEM). A low-power 638 nm laser diode illuminates the data mark pattern through the beam splitters and objective lens. Fluorescent light with a center wavelength of 650 nm is directed through the first beam splitter and off the second beam splitter to the detector.

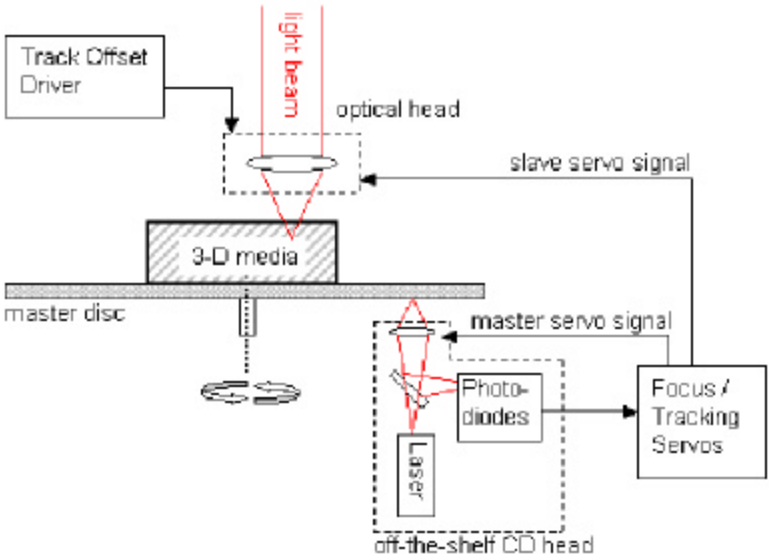

Fig 16 Layout of AEM "slave servo" concept. A master disk is used to provide a reference signal for the slave actuator in the optical head that focuses laser light into the three-dimensional medium.

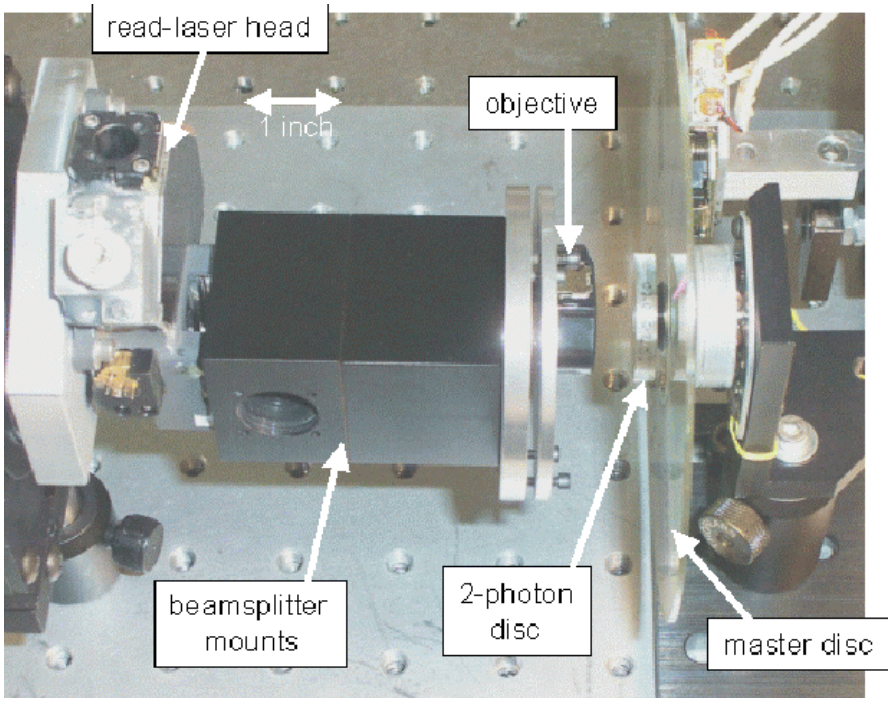

Fig 17 The AEM prototype head is a modified commercial head with beamsplitters housed in the rectangular mounts between the read-laser head and the slave-servo objective lens.